JOURNAL OF NANO- AND ELECTRONIC PHYSICS
Vol. **5** No 2, 02026(6pp) (2013)

ЖУРНАЛ НАНО- ТА ЕЛЕКТРОННОЇ ФІЗИКИ
Том **5** № 2, 02026(6cc) (2013)

X-ray Peak Broadening Analysis and Optical Studies of ZnO Nanoparticles Derived by Surfactant Assisted Combustion Synthesis

V. Sesha Sai Kumar, K. Venkateswara Rao*

Centre for Nano Science and Technology, I.S.T, Jawaharlal Nehru Technological University Hyderabad, Hyderabad-500 085 Andhra Pradesh, India

(Received 15 February 2013; published online 04 May 2013)

In this paper, synthesis of ZnO nanoparticles is done by a simple and facile surfactant assisted combustion synthesis. The synthesis of ZnO nanoparticles has been prepared using Zinc nitrate as a precursor material, glycine as a fuel with the support of non-ionic surfactant TWEEN 80. The obtained ZnO nanoparticles have been studied using characterization techniques like X-ray diffraction (XRD), Transmission Electron Microscopy (TEM), and UV-Vis Spectroscopy. XRD results reveal that the sample is crystalline with a hexagonal wurtzite phase. X-ray peak broadening analysis was used to evaluate the crystallite sizes and lattice strain by the Williamson-Hall (W-H) analysis. Further appropriate physical parameters such as strain, stress, and energy density values were also calculated using W-H analysis with different models, viz, uniform deformation model, uniform deformation stress model and uniform deformation energy density model. Transmission electron microscopy (TEM) result reveals that the ZnO nanoparticles sample is spherical in shape showing particle sizes less than 40 nm. The optical properties of ZnO nanoparticles were studied by UV-Vis spectroscopy.

Keywords: Surfactant assisted combustion synthesis, X-ray diffraction (XRD), UV-Vis spectroscopy, Transmission electron microscope (TEM).

PACS numbers: 81.07.Bc, 81.20.Ka, 61.05.C, 68.37.Lp

1. INTRODUCTION

Zinc oxide (ZnO) has recently paying attention due to its various applications such as UV light emitting diodes, varistors, gas sensors and catalysts. Zinc oxide (ZnO) is an *n*-type metal oxide semiconductor with a wide band-gap energy (~ 3.36 eV) and large exciton binding energy (~ 60 meV) at room temperature [1-5]. Therefore, many methods, including sol-gel [6], hydrothermal [7], precipitation [8], sonochemical [9], and others, have been developed to prepare ZnO nanostructures and ceramics. ZnO is the richest family of nanostructures among all semiconducting materials, both in structures and in properties due to its unique properties.

A perfect crystal would extend in all directions to infinity, so no crystals are perfect due to their finite size. This deviation from perfect crystallinity leads to a broadening of the diffraction peaks. The two main properties extracted from peak width analysis are the crystallite size and lattice strain. Crystallite size is a measure of the size of coherently diffracting domain. The crystallite size of the particles is not generally the same as the particle size due to the presence of polycrystalline aggregates [10]. The most common techniques used for the measurement of particle size, rather than the crystallite size, are the Brunauer Emmett Teller (BET), light (laser) scattering experiment, scanning electron microscopy (SEM) and TEM analysis. Lattice strain is a measure of the distribution of lattice constants arising from crystal imperfections, such as lattice dislocation. The other sources of strain are the grain boundary triple junction, contact or sinter stresses, stacking faults, coherency stresses etc. [11]. X-ray line broadening is used for the investigation of dislocation distribution. Crystallite size and lattice strain affect the Bragg peak in different ways. Both these effects increase the peak width, the intensity of the peak and shift the 2θ peak position accordingly. W-H analysis is a simplified integral breadth method where, both size induced and strain induced broadening are deconvoluted by considering the peak width as a function of 2θ [12]. Although X-ray profile analysis is an average method, they still hold an unavoidable position for grain size determination, apart from TEM micrographs.

In this work, we have synthesized ZnO nanoparticles by an easy and novel surfactant assisted combustion synthesis using oxidizer zinc nitrate with a combination fuels glycine and TWEEN 80. It was found that this method is quick, mild, and energy-efficient and eco-friendly route to produce ZnO nano particles.

In addition, a comparative evaluation of the mean particle size of the ZnO nanoparticles obtained from direct TEM measurements and from powder XRD procedures is reported. The strain associated with the as-prepared and calcined ZnO samples at 500 °C due to lattice deformation was estimated by a modified form of W-H, namely, uniform deformation model (UDM). The other modified models, such as uniform deformation stress model (UDSM) and uniform deformation energy density model (UDEDM), gave an idea of the stress-strain relation and the strain as a function of energy density 'u'. In UDM, the isotropic nature of the crystal is considered, whereas UDSM and UDEDM assume that the crystals are of an anisotropic nature. Also optical properties were studied using UV-Vis spectroscopy.

* kalagadda2003@gmail.com

2. EXPERIMENTAL

2.1 Synthesis of ZnO Nanoparticles

Zinc Oxide nano powder is synthesized by surfactant assisted combustion synthesis using $Zn(NO_3)_2.9H_2O$ and Glycine with TWEEN 80 added as a combination fuel to the above metal nitrates in 1 : 1 molar ratios following the balanced equation based on rocket fuel chemistry. This solution was then heated on a hot plate until all the liquid is evaporated. The solution containing the above redox mixture boils, foams, catches fire and burns with a smoldering flame leaving final powdered ZnO nanoparticles at the base of the beaker.

$$19.2Zn(NO_3)_3 + 7C_2H_5NO_2 + 3C_8H_{11}N \rightarrow$$
$$19.2ZnO + 38CO_2 + 34H_2O + 24.2N_2$$

The above reaction is balanced according to the rocket fuel chemistry. According to rocket fuel chemistry, the valencies of the elements Carbon, Hydrogen, Nitrogen and Oxygen are given as + 4, + 1, 0 and – 2 respectively. The valency of nitrogen is taken as zero because of its convertibility into molecular nitrogen during combustion. The valencies of metal depend upon metal ions in that compound. The valency of the metal Zinc is + 2 respectively.

2.2 Characterization

XRD and TEM were used to obtain the textural parameters of the materials, such as size, shape, composition and crystal structure, in order to recognize the improved properties of as-prepared and calcined ZnO nanoparticles. XRD was performed within the range of $25° \le 2\theta \le 65°$ by XRD, Bruker D 8,Advance, Germany using CuKα as radiation (1.5406 Å) in configuration. For TEM analysis, Tecnai G2 F20 S-TWIN FEI Transmission Electron Microscope operating at 200 kV was used to examine the morphology of the calcined nanoparticles. The optical properties of the samples were characterized by UV-Vis Spectroscopy (Systronics).

3. RESULTS AND DISCUSSION

3.1 XRD Analysis

The XRD patterns of the as-prepared and calcined samples of ZnO nanoparticles in the range of $2\theta = 25°$-65° are shown in Fig. 1. All evident peaks could be indexed as the ZnO wurtzite structure (JCPDS Data Card No: 36-1415). Wurtzite lattice parameters such as the values of d, the distance between adjacent planes in the Miller indices (hkl) (calculated from the Bragg equation, $\lambda = 2d\sin\theta$), lattice constants a, b, and c, inter-planar angle and unit cell volumes were calculatedare calculated from the Lattice Geometry equation [13]. The lattice parameters of the powders calcined at different temperatures are summarized in Table 1.

$$\frac{1}{d^2} = \frac{4}{3}\left(\frac{h^2 + hk + l^2}{a^2}\right) + \frac{l^2}{c^2} \qquad (1)$$

$$V = \frac{\sqrt{3}a^2c}{2} = 0.866a^2c \qquad (2)$$

3.2 Crystallite Size and Strain

3.2.1 Scherer Method

XRD can be utilized to evaluate peak broadening with crystallite size and lattice strain due to dislocation [14]. The crystallite size of the ZnO nanoparticles was determined by the X-ray line broadening method using the Scherer equation: $D = k\lambda / \beta_D \cos\theta$, where D is the crystallite size in nanometers, λ is the wavelength of the radiation (1.54056 Å for CuKα radiation), k is a constant equal to 0.94, β_D is the peak width at half-maximum intensity, and θ is the peak position.

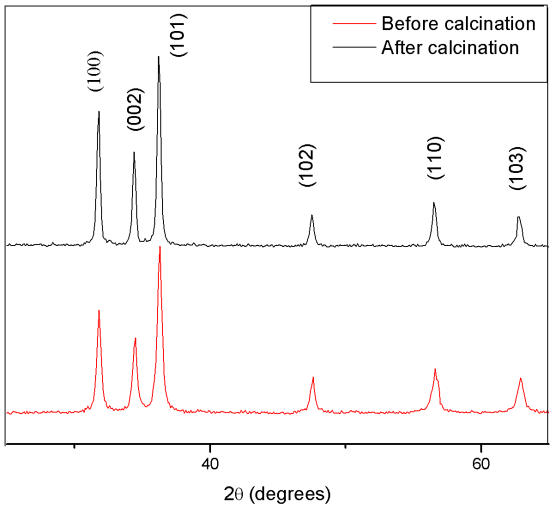

Fig. 1 – XRD pattern of ZnO nanoparticles before and after calcinations

The breadth of the Bragg peak is a combination of both instrument- and sample-dependent effects. To decouple these contributions, it is necessary to collect a diffraction pattern from the line broadening of a standard material (e.g., silicon) to determine the instrumental broadening. The instrument-corrected broadening β_D corresponding to the diffraction peak of ZnO was estimated using the relation. From the calculations, the average crystalline size of the ZnO nanoparticles before calcination is 18.9 nm and after calcination is 25.5 nm.

$$\beta_D^2 = \left[(\beta)^2_{measured} - (\beta)^2_{instrumental}\right] \qquad (3)$$

3.2.2Williamson- Hall Method

Strain-induced broadening arising from crystal imperfections and distortions are related to $\varepsilon = \beta_S / \tan\theta$. A significant property of Equation is the dependency on the diffraction angle θ. The Williamson-Hall method does not follow a $1 / \cos\theta$ dependency as in the Scherrer equation but instead varies with $\tan\theta$ .This fundamental difference allows for a separation of reflection broadening when both microstructural causes-small crystallite size and microstrain-occur together. The distinct θ dependencies of both effects laid the basis for

the separation of size and strain broadening in the analysis of Williamson and Hall [15]. Addition of the Scherrer equation and $\varepsilon = \beta_S / \tan\theta$ results in the following equations:

$$\beta_{hkl} = \beta_S + \beta_D \tag{4}$$

$$\beta_{hkl} = \left(\frac{k\lambda}{D\cos\theta}\right) + \left(4\varepsilon\tan\theta\right) \tag{5}$$

$$\beta_{hkl}\cos\theta = \left(\frac{k\lambda}{D}\right) + \left(4\varepsilon\sin\theta\right) \tag{6}$$

The above equation represents Uniform Deformation Model, where the strain was assumed to be uniform in all crystallographic directions, thus considering the isotropic nature of the crystal, where all the material properties are independent of the direction along which they are measured. The term ($\beta\cos\theta$) was plotted with respect to ($4\sin\theta$) for the preferred orientation peaks of ZnO nanoparticles with the wurtzite hexagonal phase. Accordingly, the slope and y-intersect of the fitted line represent strain and crystallite size respectively.

In the Uniform Stress Deformation Model, USDM, a generalized Hooke's law refers to the strain, keeping only the linear proportionality between the stress and strain as given by $\sigma = Y\varepsilon$, where σ is the stress of the crystal and Y is the modulus of elasticity or Young's modulus. This equation is just an approximation that is valid for a significantly small strain. Assuming a small strain to be present ZnO nanoparticles, Hooke's law can be used here. With a further increase in the strain, the particles deviate from this linear proportionality. Applying the Hooke's law approximation to the above eq. yields:

$$\beta_{hkl}\cos\theta = \left(\frac{k\lambda}{D}\right) + \left(\frac{4\sigma\sin\theta}{Y_{hkl}}\right) \tag{7}$$

For a hexagonal crystal, Young's modulus is given by the following relation [16]:

$$Y_{hkl} = \left[h^2 + \frac{(h+2k)^2}{2} + \left(\frac{al}{c}\right)^2\right]^2 \times$$
$$\times\left[S_{11}\left(h^2 + \frac{(h+2k)^2}{2}\right)^2 + S_{33}\left(\frac{al}{c}\right)^2 + \right.$$
$$\left. + \left(2S_{13} + S_{44}\right)\left(h^2 + \frac{(h+2k)^2}{2}\right)^2\left(\frac{al}{c}\right)^2\right] \tag{8}$$

where S_{11}, S_{13}, S_{33}, S_{44} are the elastic compliances of ZnO with values of 7.858×10^{-12}, -2.206×10^{-12}, 6.940×10^{-12}, 23.57×10^{-12} m^2·N^{-1}, respectively [17]. Young's modulus, Y, for hexagonal ZnO nanoparticles was calculated as ~ 127 GPa. Plots were drawn with ($4\sin\theta$) / Y_{hkl} on the x-axis and $\beta_{hkl}\cos\theta$ on the y-axis for the ZnO-nanoparticles before and after calcinations. The USDM plots for ZnO nanoparticles before and after calcinations at 500 °C are shown in Fig. 3.

The stress calculated from the slope of the fitted line is greater for the ZnO nanoparticles before calcination than for those for after calcination at 500 °C. There is another model that can be used to determine the energy density of a crystal called the Uniform Deformation Energy Density Model, UDEDM.

In Equation (9), the crystals are assumed to have a homogeneous, isotropic nature. However, in many cases, the assumption of homogeneity and isotropy is not justified. Moreover, the constants of proportionality associated with the stress -strain relation are no longer independent when the strain energy density u is considered. For an elastic system that follows Hooke's law, the energy density u (energy per unit) can be calculated from $u = (\varepsilon^2 Y_{hkl}) / 2$. Then Equation (9) can be rewritten according the energy and strain relation

$$\beta_{hkl}\cos\theta = \left(\frac{k\lambda}{D}\right) + \left(4\sin\theta\left(\frac{2u}{Y_{hkl}}\right)^{\frac{1}{2}}\right). \tag{9}$$

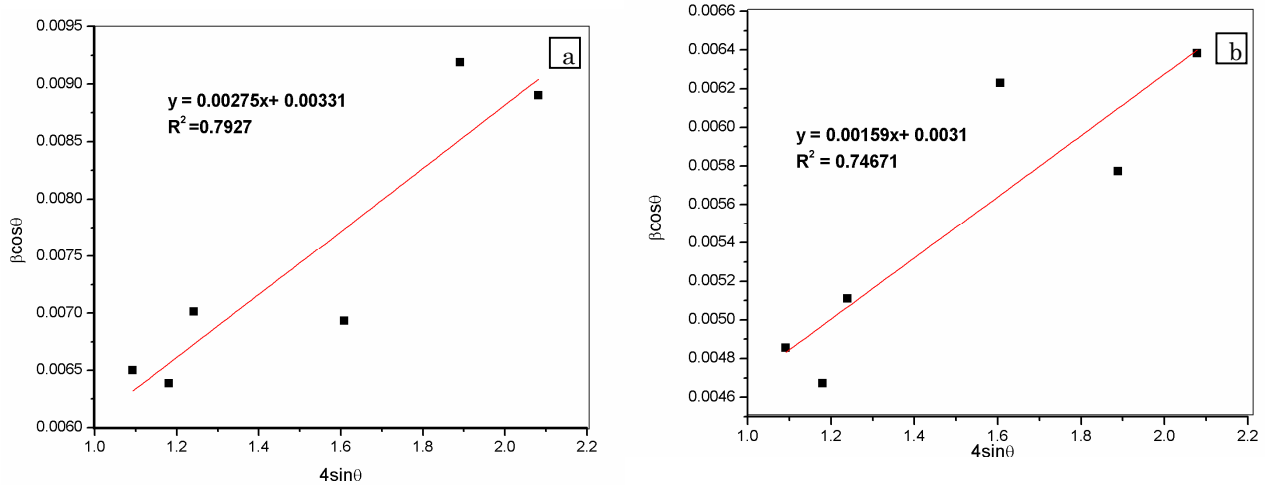

Fig. 2 – The W-H analysis of ZnO nanoparticles before and after calcinations assuming UDM

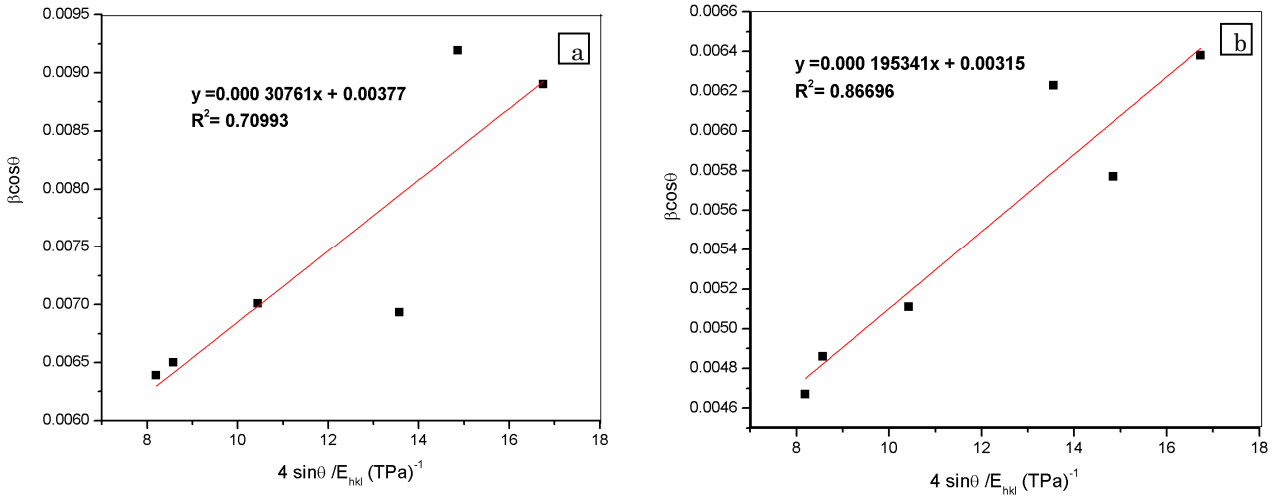

Fig. 3 – Modified form of W-H analysis assuming USDM for ZnO nanoparticles before calcinations and after calcinations

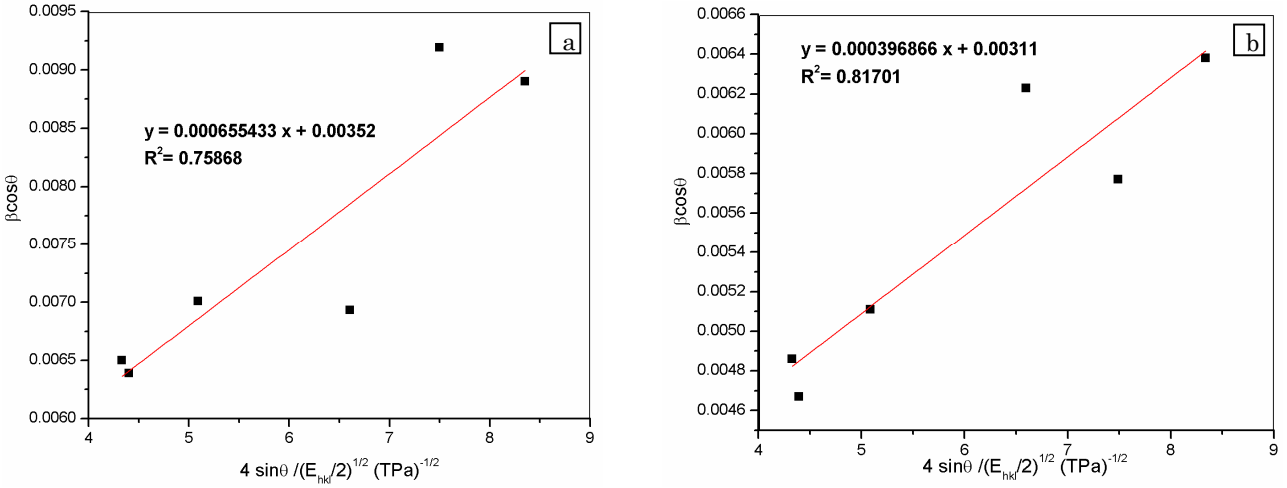

Fig. 4 – The modified form of W-H analysis assuming UDEDM ZnO nanoparticles before and after calcinations

Table 1 – The structure parameters of ZnO nanoparticles before and after calcination at 500 °C

Sample	2θ	hkl	d_{hkl} (Å)	Structure	Lattice Parameters (Å)	V (Å^3)
ZnO (as-made)	31.79 34.45	(100) (002)	2.8191 2.6073	Hexagonal	a = 3.2552 c = 5.2145 c / a = 1.6019	47.83
ZnO (500 °C)	31.76 34.40	(100) (002)	2.8224 2.6112	Hexagonal	a = 3.2590 c = 5.2222 c/a = 1.6023	48.03

Table 2 – The geometric parameters of ZnO nanoparticles before and after calcination at 500 °C

Sample	Scherer method	Williamson-method UDM		USDM			USDM			
	D nm	D nm	$\varepsilon \times 10^{-3}$	D nm	$\varepsilon \times 10^{-3}$	σ (MPa)	D nm	$\varepsilon \times 10^{-3}$	σ (MPa)	u (KJm^{-3})
ZnO (as-made)	18.90863	41.87	2.75	35.72	2.925	371.51	39.75	2.072	263.18	27.27
ZnO (500 °C)	25.55177	44.71	1.59	44	1.538	195.34	44.57	1.255	159.381	100.01

Plots of $\beta_{hkl}\cos\theta$ versus $4\sin\theta(2u / Y_{hkl})^{1/2}$ were constructed and the data fitted to lines. The anisotropic energy density u was estimated from the slope of these lines, and the crystallite size D from the y-intercept; see Fig. 4.

Previously, we had $\sigma = Y\varepsilon$ and $u = (\varepsilon^2 Y_{hkl}) / 2$ where the stress s was calculated as $u = (\sigma^2 / 2Y_{hkl})$. The results of these plots show a slight change in energy den-

sity of the ZnO nanoparticles with calcination temperature. Table 2 reviews the geometric parameters of ZnO nanoparticles before and after calcinations at 500 °C obtained from Scherrer's formula, various modified forms of W-H analysis.

3.3 Transmission Electron Microscopy

In TEM, electron beams focused by electromagnetic lines are transmitted through a thin sample of ZnO nanopowders. Fig. 5 and 6 display the TEM image and selected area electron diffraction (SAED) pattern of ZnO nanoparticles before calcination and after calcination. The average size of the ZnO nanoparticles is observed to be less than 40 nm in TEM analysis and clearly indicates that the ZnO nanoparticles are crystalline with a wurtzite structure, and no other impurities were observed. This is in close agreement with the results obtained from powder XRD data. In addition, the rings with a dotted pattern in SAED confirm the wide size distribution of ZnO nanoparticles.

3.4 UV-Vis Spectroscopy

The electronic absorption spectrum of ZnO samples in the UV-vis range enables to characterize the absorption edge related to semiconductor band structure. Fig. 7 shows the UV-visible spectra of ZnO nanoparticles synthesized by surfactant assisted combustion synthesis. The optical absorption coefficient $\alpha(\lambda)$ has been evaluated [18] from the measured spectral extinction coefficient, $k(\lambda)$, using the following expression:

$$\alpha(\lambda) = 4\pi k(\lambda) \qquad (10)$$

where λ is the wavelength of the absorbed photon.

The direct band gap energy (E_g) for the ZnO nanoparticles is determined by fitting the reflection data to the direct transition equation $\alpha h\nu = A\,(h\upsilon - E_g)^n$, where α is the optical absorption coefficient, $h\upsilon$ is the photon energy, E_g is the direct band gap and A is a constant and 'n' depends on the kind of optical transition that

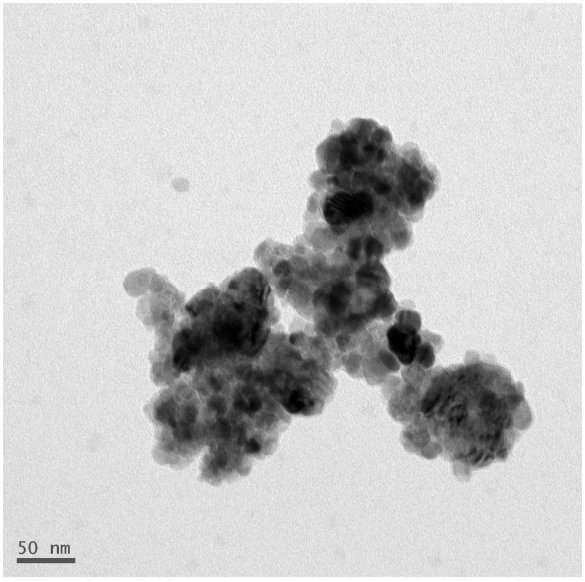

Fig. 5 – TEM pictures of as-prepared ZnO nanoparticles

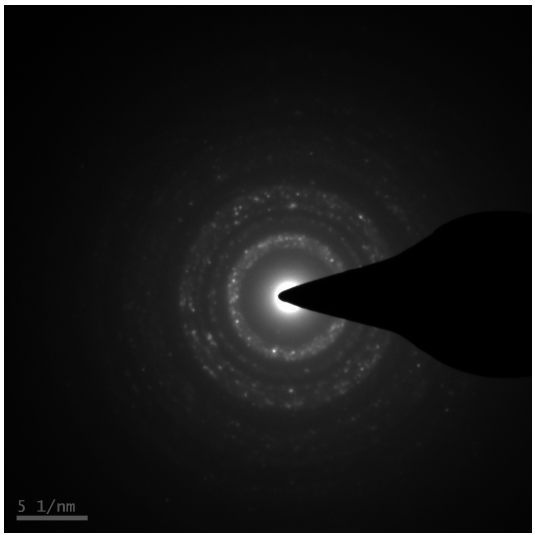

Fig. 6 – SAED pattern of as-prepared ZnO nanoparticles

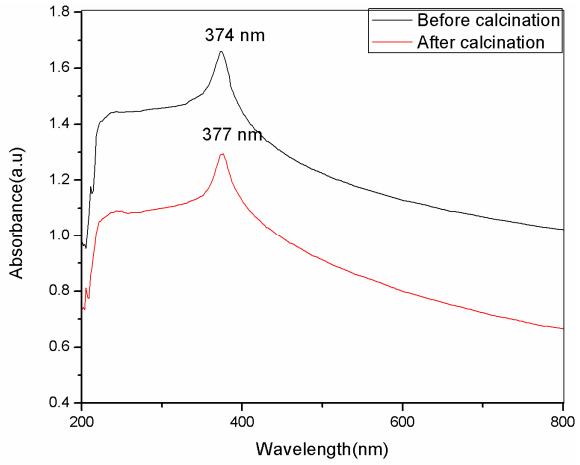

Fig. 7 – UV-vis absorption spectra of ZnO nanoparticles before and after calcinations

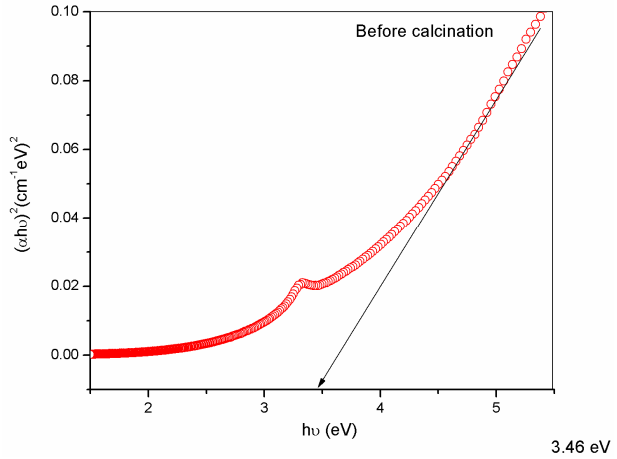

Fig. 8 – Band gap energy of ZnO nanoparticles before calcination

prevails. Specifically, with $n = 1/2$, a good linearity has been observed for the direct allowed transition, the most preferable one in the system studied here. The exact value of the band gap is determined by extrapolating the straight line portion of $(\alpha h\nu)^2$ *vs* $h\nu$ to the x-axis. The direct band gap is found to be 3.3 eV before

calcination and 3.46 eV after calcinations for ZnO nanoparticles which are shown in Fig. 8 and Fig. 9. An increase in the band gap is observed due to the quantum confinement effects in the ZnO nano particles. A typical exciton absorption at 374 nm and 377 nm is also observed in the absorption spectrum corresponds to ZnO nanoparticles before and after calcinations respectively.

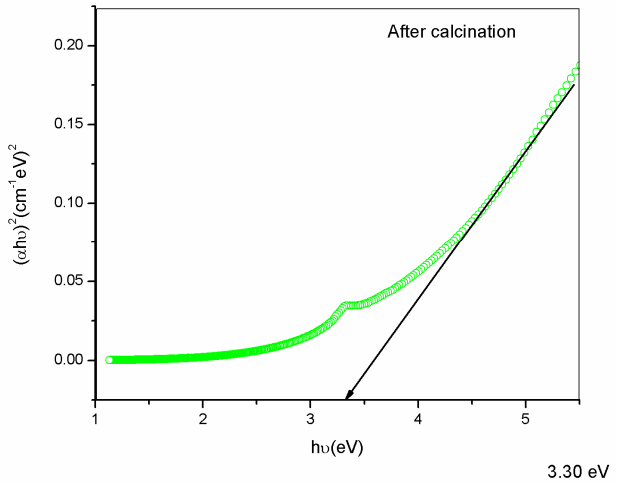

Fig. 9 – Band gap energy of ZnO nanoparticles after calcinations

4. CONCLUSIONS

ZnO nanoparticles were synthesized by surfactant assisted combustion synthesis process and characterized by XRD, TEM and UV-Vis Spectroscopy. The line broadening of ZnO nanoparticles due to the small crystallite size and strain was analyzed by Scherrer's formula. The size and strain contributions to line broadening were analyzed by the method of Williamson and Hall using uniform deformation, uniform deformation stress, and uniform deformation energy density models. From the results, it was observed that the strain value decreased but the particle size increased as calcinations temperature was increased.TEM image of calcined ZnO nanoparticles reveals the nanocrystalline nature, and their particle size is found to be less than 40 nm. The value of crystallite size calculated from the W-H analysis is in agreement with that of the average crystallite size measured from TEM.

In UV Vis spectroscopy, typical exciton absorption at 374 nm and 377 nm is observed in the absorption spectrum corresponds to ZnO nanoparticles before and after calcinations respectively, also observed the band gaps for ZnO nanoparticles as 3.3 eV before calcination and as 3.46 eV after calcinations.

REFERENCES

1. Yoshitake Masuda, Naoto Kinoshita,Fuyutoshi Sato, Kunihito Koumoto, *Cryst. Growth Des.* **6**, 75 (2006).
2. M. Singhai, V. Chhabra, P. Kang, D.O. Shah, *Mater. Res. Bull.* **32**, 239 (1997).
3. Hongyan Xu, Xiulin Liu, Deliang Cui, Mei Li, Minhua Jiang, *Sensor. Actuat. B* **114**, 301 (2006).
4. M.S. Tokumoto, S.H. Pulcinelli, C.V. Santilli, V. Briois, *J. Phys. Chem. B* **107**, 568 (2003).
5. N.S. Minimala, A. John Peter, *J. Nano- Electron. Phys.* **4** No 4, 04004 (2012)
6. A. Muthuvinayagam, Boben Thomas, P. Dennis Christy, R. Jerald Vijay, T. Manovah David, P. Sagayaraj, *Arch. App. Sci. Res.* **3**, 256 (2011).
7. Sunandan Baruah, Joydeep Dutta, *Sci. Technol. Adv. Mater.* **10**, 013001 (2009).
8. Ruby Chauhan, Ashavani Kumar, Ram Pal Chaudhary, *J. Optoelectron. Biomedical Mater.* **3**, 17 (2011).
9. Priya Mishra, Raghvendra S Yadav, Avinash C. Pandey, *Digest J. Nanomater. Bios.* **4**, 193 (2009).
10. K. Ramakanth, *Basics of X-ray Diffraction and its Application* (I.K. International Publishing House Pvt. Ltd.: New Delhi: 2007).
11. T. Ungar, *J. Mater. Sci,* **42**, 1584 (2007).
12. C. Suryanarayana, M. Grant Norton, *X-ray Diffraction: A Practical Approach* (New York: 1998).
13. B.D. Cullity, *Elements of X-ray Diffraction* (Addison-Wesley Publishing Company Inc.: California: 1956).
14. R. Yogamalar, R. Srinivasan, A. Vinu, K. Ariga, A.C. Bose, *Solid State Commun.* **149**, 1919 (2009).
15. M. Birkholz, *Thin Film Analysis by X-ray Scattering* (Wiley-VCH Verlag GmbH and Co.: KGaA, Weinheim: 2006).
16. J. Zhang, Y. Zhang, K.W. Xu, V. Ji, *Solid State Commun.* **139**, 87 (2006).
17. J.F. Nye, *Physical Properties of Crystals: Their Representation by Tensors and Matrices* (Oxford: New York: 1985).
18. J. Tauc, *Amorphous and Liquid Semiconductors*, (Plenum: New York: 1974).